Time of Flight Measurements for Optically Illuminated Underwater Targets Using Compressive Sampling and Sparse Reconstruction

Robert Lee[1,2]
Dr. Linda Mullen[1]
[1]Naval Air Systems Command
Patuxent River, MD, USA
robert.lee9@navy.mil

Dr. Piya Pal[2]
[2]University Of Maryland, College Park
Electrical Engineering Dept.
College Park, MD, USA

David Illig[3]
[3]Clarkson University
Electrical Engineering Dept.
Potsdam, NY, USA

***Abstract*—Compressive Sampling and Sparse reconstruction theory is applied to a linearly frequency modulated continuous wave hybrid lidar/radar system. The goal is to show that high resolution time of flight measurements to underwater targets can be obtained utilizing far fewer samples than dictated by Nyquist sampling theorems. Traditional mixing/down-conversion and matched filter signal processing methods are reviewed and compared to the Compressive Sampling and Sparse Reconstruction methods. Simulated evidence is provided to show the possible sampling rate reductions, and experiments are used to observe the effects that turbid underwater environments have on recovery. Results show that by using compressive sensing theory and sparse reconstruction, it is possible to achieve significant sample rate reduction while maintaining centimeter range resolution.**

Keywords—FMCW Lidar; Compressive Sampling; Sparse Reconstruction; Frequency Chirp;

I. Introduction

Accurately measuring an object's range relies on calculating the Time of Flight (ToF) between when a signal was transmitted and subsequently received after roundtrip propagation. A linearly Frequency Modulated Continuous Wave (FMCW) waveform, also known as a chirp, is a class of signals where the time-shifted spectral content can be used to determine the range to an illuminated object [1, 2]. While traditionally used in Radar/Sonar applications, this class of waveforms can also be applied to lidar systems which have the benefits of a highly directive illumination source that can be modulated with wide bandwidth radar waveforms. An additional benefit is that by encoding a blue-green laser with a radar waveform, radar modulation, demodulation, and signal processing techniques can be applied to scenarios that are typically not accessible to radar systems, such as those in the underwater environment. The underwater channel however imposes significant absorption and scattering challenges when using optical signals. Photons which are scattered back towards the receiver before ever reaching the object compete with the received signal power from the target and decrease SNR. Photons which have been scattered in the forward direction can lead to a loss of spatial resolution due to beam spreading. A subsequent increase in propagation path can also lead to pulse stretching which reduces range resolution. Research has shown that the effects of scattering and absorption can be reduced by intensity modulating blue-green laser sources at frequencies exceeding 100MHz [3]. The challenge is that as the bandwidth of these systems increase, traditional sampling theorems dictate the need for wide bandwidth digitizers to accurately capture the signal at the receiver. Therefore, the desire for modulating a laser at high frequencies and wide-bandwidths is accompanied by the need for high-speed digitizers which increase a systems cost and complexity.

To develop alternate techniques for processing wideband signals, it is important to note that the recovery of the received wideband signal is not the goal for ranging systems. The desired information of interest is the range, or equivalently the ToF, between transmitted and received signals. It has been proposed that compressive sensing theory and sparse representations can be used reduce the amount of data that needs to be collected for radar imaging systems [4, 5]. In this paper, it will be shown that under the assumption that there are a finite number of reflecting objects to be detected, compressive sampling (CS) theory and sparse recovery algorithms can be used to exploit the inherently sparse nature of FMCW lidar systems. The anticipated benefits include a lower required digitization rate which reduces the total number of samples needed to be collected without sacrificing system performance, specifically range resolution, in various underwater environments.

II. Compressive Sampling

If a signal is or can be represented by far fewer non-zero than zero elements it can be classified as a sparse or compressible signal [6, 7]. These classes of signals are characterized by their support which is defined as number of non-zero elements. Common examples include Dirac pulses which are inherently sparse, or sinusoids which are compressible in the Fourier domain. CS theory implies that by solving a convex minimization problem, it is possible to reconstruct such signals given only a small set of incoherent projections [7]. A generalization of the CS and sparse recovery

This is a DRAFT. As such it may not be cited in other works. The citable Proceedings of the Conference will be published in IEEE Xplore shortly after the conclusion of the conference.

978-0-933957-43-5 ©2015 MTS

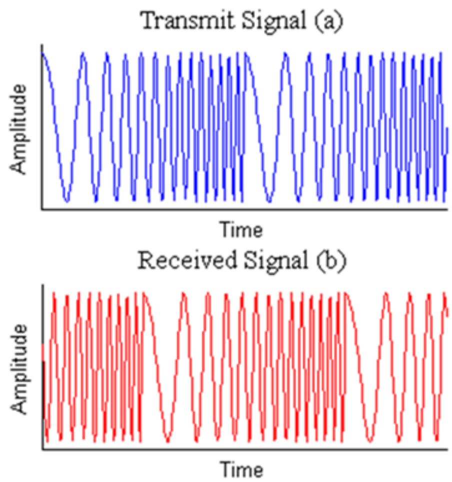

Fig. 1: (a) Signal used to intensity modulate the laser source (b) Signal Received after round trip propagating to the illuminated object

problem can be formed by first observing that a vector $\vec{x} \epsilon \mathbb{R}^N$ can be represented by projecting a sparse vector $\vec{s} \epsilon \mathbb{R}^N$ with support $K<<N$ onto a dictionary given by the N-by-N matrix Ψ. The vector $\vec{y} \epsilon \mathbb{R}^M$ is composed of a set of M linear projections, or measurements, of $\vec{x}$ where $M<N$. This measurement process is given by (1), where the matrix Φ is the M-by-N measurement matrix, and the matrix Θ is the M-by-N sensing matrix.

$$\vec{y} = \Phi\vec{x} = \Phi\Psi\vec{s} = \Theta\vec{s} \quad (1)$$

The goal of CS is the successful recovery of $\vec{s}$ given $\vec{y}$ and Θ. When the sensing matrix satisfies the *Restricted Isometry Property* (RIP) or other related *Incoherence* conditions, then it is said that with high probability that the sparse vector is recoverable [8]. This recovery is made possible through the $\ell_1$norm minimization problem given by (2) where the solution is with high probability the sparsest solution [9].

$$\hat{s} = \min\|\tilde{s}\|_{\ell_1} \text{ such that } \Theta\tilde{s} = \vec{y} \quad (2)$$

For example, when the sensing matrix is derived from Gaussian, Bernoulli, or Fourier measurements, it has been proven that exact recovery is possible from ℓ_1 norm minimization [7, 10]. One commonly used algorithm to solve the necessary minimization problem is the Orthogonal Matching Pursuit (OMP) algorithm which has been proven to perform well in the presence of noise [11], and has the potential for fast implementation [12]. The algorithm takes as its inputs the measurement vector, the sensing matrix, and the expected support of the output, and outputs an approximation of the sparsest solution.

This papers goal is to apply CS theory to linear FMCW lidar systems. In order to accomplish this goal, it is necessary to first reformulate the problem as a set of linear projections, and identify in which way the system is sparse. Then the sensing matrix must be found, and it must be determined if recovery of the range information is possible through a small set of linear measurements. These issues are discussed in more detail in the next section.

III. CS FMCW Lidar

The FMCW Lidar system to be explored is composed of a laser transmitter and an opto-electronic receiver collocated on the same platform. The transmitted optical signal $Tx(t)$ is intensity modulated with a linearly chirped waveform, shown in Fig. 1a, with a defined bandwidth (Δf) and duration (T_c). The optically illuminated scene could most generally be composed of a finite number K of reflecting objects given by (3), where α_i and τ_i are the i^{th} object's reflectivity and propagation time delay respectively.

$$s(t) = \sum_{i=1}^{K} a_i\delta(t-\tau_i) \quad (3)$$

The signal at the receiver, $Rx(t)$ Fig. 1b, can be expressed as a convolution of the target scene with the transmitted signal given by (4).

$$x(t) = \int Tx(t-\tau)s(\tau)d\tau \quad (4)$$

In traditional chirped FMCW Lidar systems there are two main methods for acquiring the ToF information. The first method, shown in Fig. 2, mixes the received signal with a transmitted signal reference, and the spectrum of the mixer output is used to determine the range to the illuminated objects [13]. This mixed signal method has a resolution which is proportional to the chirp signal's bandwidth, but requires long chirp periods to achieve low sampling rates. The second method, shown in Fig. 3, first samples the received signal at or above the Nyquist rate, F_N, using a high speed digitizer. Then, a digitized copy of the transmitted signal is used to implement a digital matched filter [14]. The output of the matched filter is processed to determine the range to an object within the illuminated scene. The matched filtering method improves upon the achievable resolution and produces an SNR enhancement due to pulse compression. However, the digitizer must now be capable of accurately sampling the chirped

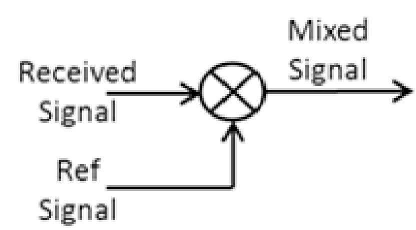

Fig. 2: Mixed signal processing method, Reference and received signal are mixed together to produce a mixed signal with spectral peaks corresponding to illuminated objects

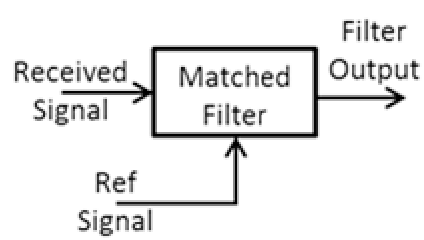

Fig. 3: Matched filter processing method. Reference signal is used to generate an ideal filter which induces pulse compression. Filter output has peaks corresponding to object locations

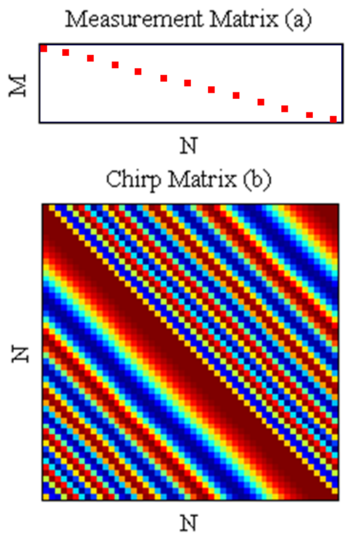

Fig.4: Illustration of the Measurement Matrix (a) which corresponds to a uniform down-sampling, and the Chirp Matrix (b). The first column on the left of (b) shows the transmitted chirp signal with low to high frequency content from the top row to the bottom. As an object moves further away this induces a circular shift of the spectral content in the transmitted signal seen as the columns are traversed from left to right.

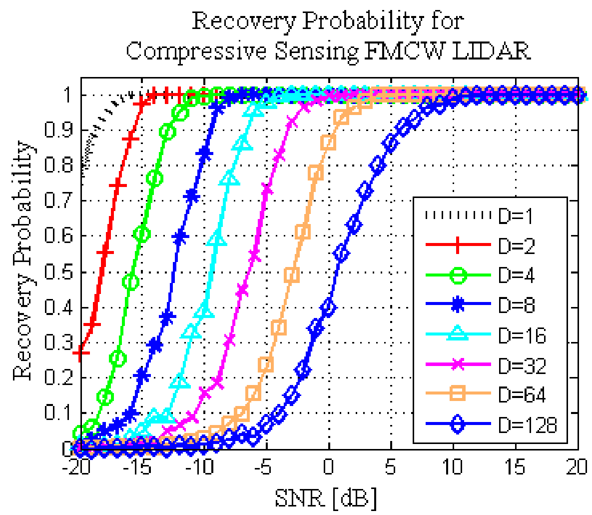

Fig. 6: Simulation results as a function of SNR and down-sampling factor. The results show under what conditions is recovery of the object vector possible for a single point reflecting object.

signal's full bandwidth.

To realize how CS theory can benefit FMCW Lidar systems, the signal at the receiver (given by Equation 4) is uniformly under-sampled at a rate F_N/D (5), where D is an down-sampling factor, $y[m]$ is the under-sampled signal, $s[n]$ is a Nyquist sampled version of $s(t)$, and N is the total number of samples over a chirp period T_c:

$$y[m] = Rx(t)|_{t=mD/F_N} \tag{5}$$

$$= \sum_{n=1}^{N} Tx[mD-n]s[n]$$

$$\vec{y} = \Phi\Psi\vec{s} \tag{6}$$

Equation (5) can be rewritten in matrix notation (6), through the following observations. First, $s[n]$ can be represented by an object vector $\vec{s}\,\epsilon\,\mathbb{R}^N$ where the non-zero elements are the discrete reflectivity values, a_i , of the illuminated objects. Second, $y[m]$ can be represented by a measurement vector $\vec{y}\,\epsilon\,\mathbb{R}^M$ where M is the number of measurements given by N/D . Lastly, the discrete convolution in (5) can be represented by a matrix multiplication between the measurement matrix Φ, and the chirp matrix Ψ. Specifically, the chirp matrix is an N-by-N toeplitz matrix with columns that are circularly shifted versions of the transmitted chirp signal, and the measurement matrix is an M-by-N decimated version of the N-by-N identity matrix. The structure and elements of the measurement and chirp matrices are shown pictorially in Figs. 4a and 4b respectively.

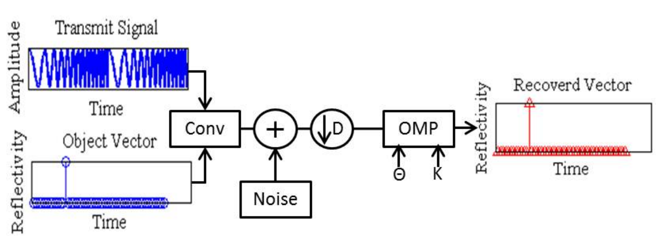

Fig. 5: Block diagram showing how the simulations were run. The received signal was simulated by convolving a linear FMCW chirp with an ideal point reflecting object. Additive white Gaussian noise was added to the simulated received signal which was then down-sampled and processed

Given the direct relationship between Equations (1) and (6), and the assumption that there are only a few reflecting objects, the FMCW Lidar problem has been reformulated in a way that represents a CS and sparse recovery problem. In many cases, due to the directive nature of laser sources, the transmitter will only be illuminating a single object thus making this assumption valid, i.e. *K=1*. Proof of the RIP or other related conditions have yet to be analytically shown for the derived deterministic sensing matrix. However, the toeplitz structure and research done in [15] provides the intuition that recovery may be possible. In the following section, simulated and experimental results will be provided which give evidence that under certain conditions, it is in fact possible to recover the sparse object vector $\vec{s}$ from this sensing system, and thus object range information can be obtained.

IV. Simulated and Experimental Results

A. *Simulated Results*

To initially show that recovery of an object's range using the above formulation is possible, an FMCW Lidar system was modeled. A Nyquist sampled chirp signal with duration 1 µsec, and bandwidth 800MHz (200-1000MHz) was generated and convolved with an object vector consisting of a single target with unit reflectivity. To generate the measurement vector, additive white Gaussian noise was added to the simulated receiver signal prior to it being resampled. For this simulation, the sample rates ranged from 2000MHz to 15.625MHz, corresponding to down-sampling factors from 1-128. The OMP algorithm, given the measurement vector, the sensing matrix, and an expected support of one, was then used to find the sparsest solution which was then compared to the original object vector. This process is highlighted in Fig. 5. To determine the recovery probability as a function of SNR and down-sampling factor, the outlined process was repeated 1000 times. Results for these simulations are show in Fig. 6 where we see that, given certain conditions, recovery of the original object vector is possible with high probability from a set of

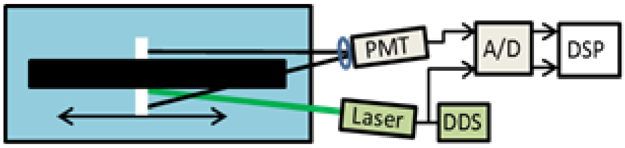

Fig. 7: Experimental setup developed to investigate the effect that propagation through a turbid underwater environment would have on compressive sampling and sparse reconstruction while also providing insight into the range resolution of different digital signal processing (DSP) schemes.

samples much smaller than the number of Nyquist samples. Specifically for a sample rate 32 times less than Nyquist these results show that exact recovery is achieved at SNR's greater than -5dB. While these results provide sufficient evidence that CS and sparse recovery is possible using FMCW Lidar systems, the underwater channel and the complications it imposes have not yet been considered.

B. Experimental Setup

An experiment was designed to determine how the underwater channel affects the application of CS to chirped FMCW lidar systems, and the setup is shown in Fig. 7. At the transmitter, an Analog devices (AD9914) Direct Digital Synthesizer (DDS) board was used to generate a 1µsec chirp signal with a frequency range of 200-1000MHz (800MHz Bandwidth). This signal was then used to intensity modulate a custom 532nm CW laser source manufactured by AdvR, Inc. The laser consisted of an infrared laser diode that was modulated by a mach zhender modulator, amplified via fiber

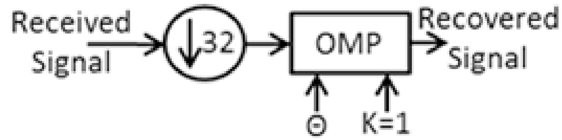

Fig. 8: Block diagram to highlight the processing steps used to recover the target's range and magnitude information. The recovered signal is a vector with only 1 non zero element. The index of this element is related to the range of the target.

amplifiers, and doubled to green. The receiver, located on the same platform as the transmitter, consisted of a high speed Photo-Multiplier Tube (PMT) and a two channel 4GSPS high speed digitizer (A/D). The laser signal was propagated through a water tank with a single target placed on a translation stage. The object's range was varied in 1cm steps from 0.80m to 2.20m away from the transmitter/receiver platform. The turbidity of the water was varied using a common scattering agent (Equate antacid) [16], and the attenuation coefficient, c [m^{-1}], was measured using a WETLabs AC-9, absorption and attenuation meter. For each turbidity level, the laser power was set to maximize the dynamic range of the PMT and the A/D when the target was at its closest position.

C. Mixed Signal, Matched Filer, and CS Processing

At each target range, the transmitted and received signals were sampled at 4GSPS and averaged over 100 chirp periods. This 100µsec integration time was used to improve SNR so that the effects of scattering could be observed even at low

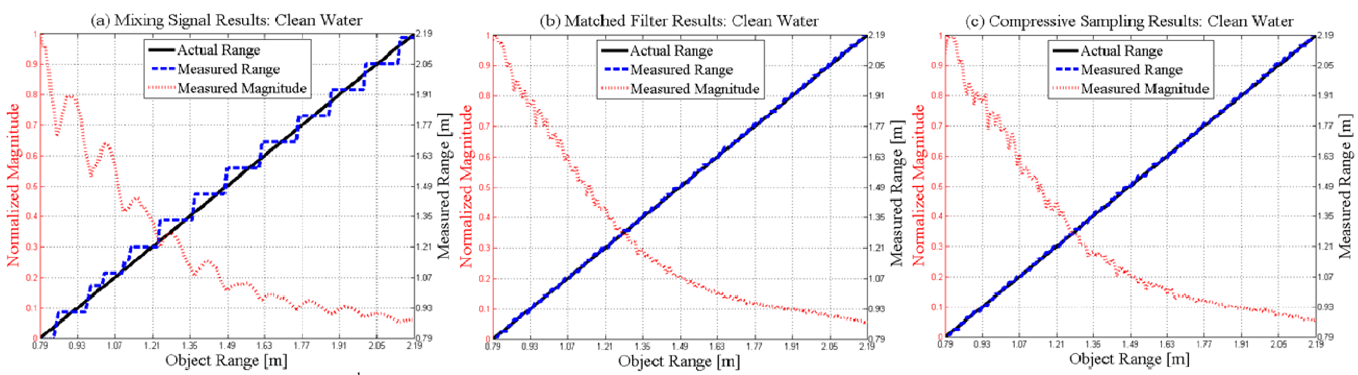

Fig. 9: Clean water results C = 0.20 m^{-1} for (a) mixed signal using a 250MHz sampling rate (b) matched filter using a 4000MHz sampling rate and (c) compressive sampling and sparse reconstruction using a 125MHz..

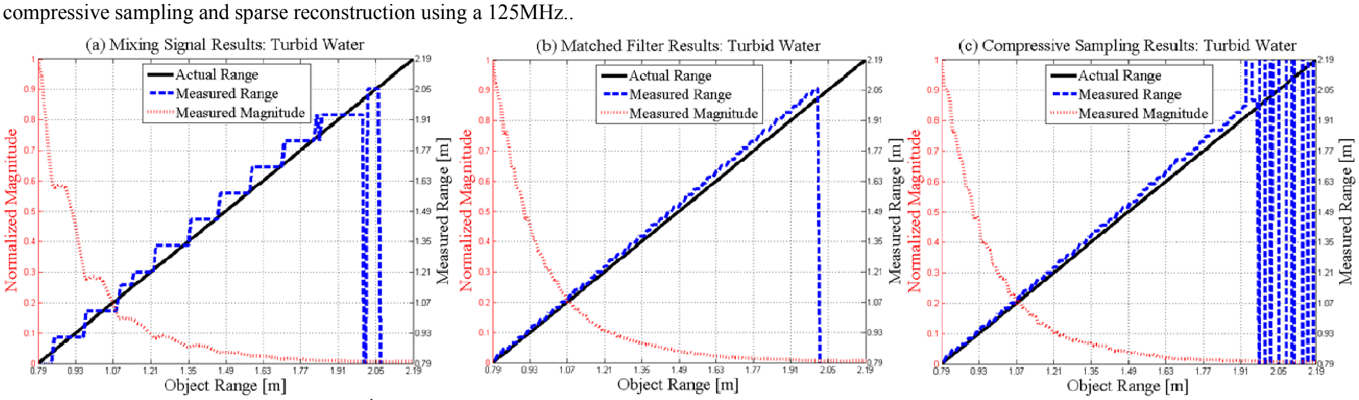

Fig. 10: Turbid water results C = 7.00 m^{-1} for (a) mixed signal using a 250MHz sampling rate (b) matched filter using a 4000MHz sampling rate and (c) compressive sampling and sparse reconstruction using a 125MHz..

signal levels when scattering losses were high. The integrated signals were processed in three different ways to obtain the magnitude of the received signal and range to the target. The first processing method, highlighted in Fig. 2, mixes the digitized transmitted and received signals, calculates the mixed signal spectrum, and then finds the peak spectral value and frequency which can then be related to the magnitude and range information, respectively. The second processing method, introduced in Fig. 3, uses the digitized transmit signal to implement a digital matched filter, where the peak value and time index of the matched filters output is proportional to the magnitude and range. The third processing method, shown in Fig. 8, was used to implement the CS and sparse recovery method. The measurement vector was created by resampling the received signal at a rate of 125MHz, corresponding to a down-sampling factor of 32. The use of averaging enhanced the SNR to >5dB ensuring that for this chosen decimation factor, we would expect to achieve a recovery probability of ~100%, as seen in Fig. 6. The sensing matrix was previously created as highlighted in Equation (5), using the known chirp parameters and down-sampling factor. To solve the ℓ_1 norm minimization problem shown in Equation (2), the OMP algorithm was implemented with an expected support of one, and the recovered value and index of the single non-zero element was used to determine magnitude and target range.

D. *Experimental Results*

For each processing method, the measured magnitudes and ranges were plotted as a function of the known target locations. The measured results for signals collected in clean water (c≈0.2 m^{-1}), are shown for the mixed signal, matched filter, and CS processing methods in Fig. 9a, 9b 9c respectively. When looking at the magnitude plots, the results show the propagation loss that is expected as the path length increases. In observing the target range measurements, the first notable result is the accurate recovery of the target's range using the compressive sensing method and a sampling rate that is a 32 times lower than needed to record the raw chirp waveform (Fig 9c). Additionally the resolution of the CS method is equivalent to that of matched filtering, and both are a significant improvement when compared to the mixed signal method. This result is to be expected given that mixed signal method suffers from a frequency binning that is proportional to the bandwidth of the transmitted chirp. When using this processing method, a range resolution of approximately 14cm is observed. For the matched filtering method, the individual time bin size is equal to the sampling period, while for the CS method, the size of a single time bin is equal to the temporal resolution of the stored sensing matrix. For the results presented here, the stored sensing matrix's temporal resolution was the same as the sampling period used in the matched filtering method leading to a range resolution of approximately 2cm.

The experiment was completed again in a significantly more turbid environment (c≈7.0 m^{-1}) to amplify the effects of scattering. Results presented in Fig. 10a, 10b, and 10c use the same order as in the previous Fig. 9. When observing the magnitude plots for all methods and comparing them to the previous clean water data, a significantly steeper exponential decay is observed due to the increased amount propagation losses due to scattering. More importantly, these figures show that the resolution of the different methods is unaffected by the turbid underwater environment, and exact recovery using CS and sparse recovery is still successful. It is also shown that, even when provided sufficient SNR through integration, all methods succumb to the effects of scattering at similar ranges. The effects of forward scattering are evident through the systematic range bias seen in the measured range for all processing methods. This is due to the effective increase in propagation path due to the small angle forward scattering which causes the measured range to be larger than the actual target range. Backscatter effects can be seen at the farthest target ranges where the measured range values no longer track the actual target range.

V. CONCLUSION

Through a reformulation of the chirped FMCW lidar problem, a detailed analysis was completed to show how compressive sampling theory and sparse recovery can be used to determine the range to illuminated objects. Using simulations it was shown that, under various SNR conditions, these methods can achieve exact recovery of an objects location using sampling rates significantly lower than the Nyquist frequency. Furthermore, through experimental evidence, it was proven that these methods can be directly applied to current FMCW lidar systems to reduce the number of samples and the rate that they must be collected. The experimental evidence was obtained in both clear and turbid underwater environments, and it was shown that resolution and operational ranges were not adversely affected when compared to more established methods. While analytical proof for exact recovery has not yet been provided, the reported empirical evidence shows the potential benefits of CS theory and sparse recovery in terms of the reducing the sampling rate requirements of the digitizer, without sacrificing system resolution or performance in turbid underwater environments.

REFERENCES

[1] Skolnik, Merrill I. Radar Handbook. New York: McGraw-Hill, 2008.

[2] Stove, A.G.: 'Linear FMCW radar techniques', IEE Proceedings F (Radar and Signal Processing), 1992, 139, (5), p. 343-350, doi:10.1049/ip-f-2.1992.0048

[3] Mullen, L.J.; Contarino, V.M., "Hybrid LIDAR-radar: Seeing through the scatter," Microwave Magazine, IEEE , vol.1, no.3, pp.42,48, Sep 2000 doi:10.1109/6668.871186

[4] Baraniuk, R.; Steeghs, P., "Compressive Radar Imaging," Radar Conference, 2007 IEEE , vol., no., pp.128,133, 17-20 April 2007 doi:10.1109/RADAR.2007.374203

[5] Herman, M.A.; Strohmer, T., "High-Resolution Radar via Compressed Sensing," Signal Processing, IEEE Transactions on , vol.57, no.6, pp.2275,2284, June 2009 doi:10.1109/TSP.2009.2014277

[6] Elad, M.; Bruckstein, A.M., "A generalized uncertainty principle and sparse representation in pairs of bases," *Information Theory, IEEE Transactions on* , vol.48, no.9, pp.2558,2567, Sep 2002 doi: 10.1109/TIT.2002.801410

[7] Candes, E.J.; Wakin, M.B., "An Introduction To Compressive Sampling," Signal Processing Magazine, IEEE , vol.25, no.2, pp.21,30, March 2008 doi:10.1109/MSP.2007.914731

[8] Baraniuk, Richard, Mark Davenport, Ronald Devore, and Michael Wakin. "A Simple Proof of the Restricted Isometry Property for Random Matrices." Constr Approx Constructive Approximation 28.3 (2008): 253-63.

[9] Donoho, David L. "For Most Large Underdetermined Systems of Linear Equations the Minimal ▪ 1-norm Solution Is Also the Sparsest Solution." Communications on Pure and Applied Mathematics Comm. Pure Appl. Math. 59.6 (2006): 797-829. doi:10.1002/cpa.20132

[10] Candes, E.J.; Romberg, J.; Tao, T., "Robust uncertainty principles: exact signal reconstruction from highly incomplete frequency information," Information Theory, IEEE Transactions on , vol.52, no.2, pp.489,509, Feb.2006doi:10.1109/TIT.2005.862083

[11] Cai, T.T.; Lie Wang, "Orthogonal Matching Pursuit for Sparse Signal Recovery With Noise," Information Theory, IEEE Transactions on , vol.57,no.7,pp.4680,4688July2011

[12] Sung-Hsien Hsieh; Chun-Shien Lu; Soo-Chang Pei, "Fast OMP: Reformulating OMP via iteratively refining ℓ2-norm solutions," Statistical Signal Processing Workshop (SSP), 2012 IEEE , vol., no., pp.189,192,5-8Aug.2012

[13] Illig, David W., Laux, Alan; Lee, Robert; Jemison, William; Mullen, Linda;. "FMCW Optical Ranging Technique in Turbid Waters." Ocean Sensing and Monitoring VII (2015) doi:10.1117/12.2177051.

[14] O'connor, Shawn; Lee, Robert;, Mullen, Linda;, and Brandon Cochenour. "Waveform Design Considerations for Modulated Pulse Lidar." Ocean Sensing and Monitoring VI (2014) doi:10.1117/12.2050395

[15] Bajwa, W.U.; Haupt, J.D.; Raz, Gil M.; Wright, S.J.; Nowak, R.D., "Toeplitz-Structured Compressed Sensing Matrices," Statistical Signal Processing, 2007. SSP '07. IEEE/SP 14th Workshop on , vol., no., pp.294,298, 26-29 Aug. 2007 doi:10.1109/SSP.2007.4301266

[16] Mullen, Linda; Alley, Derek; Cochenour Brandon; "Investigation of the effect of scattering agent and scattering albedo on modulated light propagation in water," Appl. Opt. 50, 1396-1404 (2011) doi: 10.1364/AO.50.0013